

HU-SEFT R 1996-19  
27 September 1996

## B-physics potential of ATLAS: an update

P. Eerola <sup>1</sup>  
*CERN, Geneva, Switzerland*

For the ATLAS Collaboration

### Abstract

The B-physics potential of the ATLAS experiment at LHC is described. Simulation results are shown for the measurement of  $\sin 2\beta$ , with an emphasis on new tagging techniques. Other CP-violation measurements are described briefly. New limits are shown for the reach of the  $x_s$ -measurement, resulting from increased statistics and improved fitting methods. Some rare decay modes of B-mesons can be easily seen in ATLAS. Analyses of channels  $B \rightarrow \mu^+ \mu^- (X)$  are presented here.

*Presented in BEAUTY'96, June 17-21 1996, Rome, Italy.  
To be published in Nucl. Instrum. and Methods A.*

---

<sup>1</sup>On leave of absence from SEFT and University of Helsinki, Helsinki, Finland

# 1 B physics in ATLAS

LHC is a B-factory. At  $\sqrt{s} = 14$  TeV, the cross-section for  $b\bar{b}$  production is about  $500 \mu b$ , with  $\sigma(b\bar{b})/\sigma(\text{tot}) \simeq 0.7\%$ . At the start-up of LHC, the luminosity is expected to be  $\mathcal{L} = 10^{33} \text{ cm}^{-2}\text{s}^{-1}$ , corresponding to an integrated luminosity of  $10^4 \text{ pb}^{-1}$  per year giving  $5 \cdot 10^{12} b\bar{b}$  pairs.

ATLAS can measure precisely CP-violation in the decay  $B_d^0 \rightarrow J/\psi K_S^0$ , which measures the  $\beta$ -angle in the unitarity triangle, and  $B_s^0$ -mixing, which measures the length of the side opposite to  $\gamma$ -angle. With these two measurements, the triangle is already completely defined according to the Standard Model. In order to test the Standard Model, one needs additional experimental (over)constraints. ATLAS can contribute to measurements of the other two angles,  $\alpha$  and  $\gamma$ . In addition, rare decays provide us with an independent Standard Model test.

The ATLAS B-physics reach has been previously studied in [1] and in [2]. These publications also include detailed descriptions of the ATLAS detector and formulae for CP-violation measurements. Here, we concentrate on new simulation results. New tagging techniques for the measurement of  $\sin 2\beta$  are described in detail. An improved limit for the  $x_s$ -reach is obtained, due to increased signal statistics (decay channels  $B_s^0 \rightarrow D_s^- \pi^+$  and  $B_s^0 \rightarrow D_s^- a_1^+$ ), and refined fitting methods. New analyses on rare decays  $B \rightarrow \mu^+ \mu^- (X)$  are presented in some detail in this paper.

# 2 The ATLAS experiment

ATLAS is a general purpose experiment at LHC [1]. The new particle searches at the nominal LHC luminosity ( $\mathcal{L} = 10^{34} \text{ cm}^{-2}\text{s}^{-1}$ ) have defined most of the performance specifications of the detector. B-physics requirements have been accommodated, however, in particular in the design of the inner detector and the trigger systems.

The inner detector, located in a 2 T solenoidal field, consists of a semiconductor tracker (SCT), providing at least six high-precision space points over pseudorapidity range of  $\pm 2.5$ , and a transition radiation tracker (TRT) providing on the average 35 two-dimensional measurement points over  $|\eta| < 2.5$ . Electrons with  $p_T > 1 \text{ GeV}/c$  can be identified by the transition radiation they produce in the TRT. For the initial low-luminosity operation of LHC, ATLAS will also be equipped with a special vertexing layer next to the beam pipe, either a pixel or a double-sided strip layer. The nominal resolutions of the strip layer are  $\sigma_{\text{IP}} = (13 \oplus 58/(p_T \sqrt{|\sin \theta|})) \mu\text{m}$ ,  $\sigma_z = (37 \oplus 62/(p_T \sqrt{|(\sin \theta)^3|})) \mu\text{m}$ , where  $\sigma_{\text{IP}}$  is the resolution in the transverse plane,  $\sigma_z$  is the resolution in  $z$ ,  $p_T$  is given in  $\text{GeV}/c$ , and  $\theta$  is the polar angle.

Muons with  $p_T > 5 \text{ GeV}/c$  are identified in the muon spectrometer, which is a large toroid-system equipped with muon chambers and dedicated trigger chambers. In addition, the last compartment of the barrel hadron calorimeter can be used for identifying muons with  $p_T > 3 \text{ GeV}/c$ . The low- $p_T$  electron identification used here relies on the TRT, but preliminary studies show that electrons in b-jets can also be identified in the Liquid-argon

calorimeter with  $p_T$  values as low as  $2 \text{ GeV}/c$  [3].

The B-physics Level-1 trigger is a single muon trigger with  $p_T > 6 \text{ GeV}/c$ ,  $|\eta| < 2.2$ . At Level-1, the total rate is about 8 kHz, with 60% b-purity (60%  $b\bar{b}$ , 20%  $c\bar{c}$ , 20%  $\pi/K$  decays). The  $p_T$  measurement of the trigger muon will be refined in Level-2. In addition, more elaborate signatures will be used at Levels 2 and 3, requiring for example additional leptons, additional high- $p_T$  tracks, or making mass cuts.

### 3 Measurement of $\sin 2\beta$

The CP-violation parameter  $\sin 2\beta$  is measured from the asymmetry of the decays ( $B_d^0 \rightarrow J/\psi K_S^0$ ) and ( $\bar{B}_d^0 \rightarrow J/\psi K_S^0$ ). To distinguish B- and  $\bar{B}$ -decays, a tag is used. In ATLAS, the tag can be charge of the lepton, which originates from a semileptonic decay of the other B,  $b \rightarrow \ell^-$ . We have also investigated  $B^{**}$ -tagging, in which the charge of the pion next to the signal-B provides the tag, and jet charge tagging, in which the charge of the jet containing the signal-B, or the charge of the other B-jet, or a combination of the two, provides the tag.

The asymmetry is reduced by wrong tags (dilution factor  $D_{\text{tag}} = 1 - 2W_{\text{tag}}$ ,  $W_{\text{tag}}$  = wrong tag fraction) and background (dilution factor  $D_{\text{back}} = N_S/(N_S + N_B)$ ). If a time-independent measurement of the asymmetry is performed, the time-integration produces an effective dilution factor  $D_{\text{int}} = 1/(1 + x_d^2)[\sin \Delta m t_0 + x_d \cos \Delta m t_0]$ , where  $x_d = \Delta m/\Gamma$  is the mixing parameter, and  $t_0$  is the starting point for the time-integration. With a time-dependent measurement of the asymmetry, a better precision can be obtained, with a dilution factor  $D_{\text{time}}$  from the fitting procedure. In addition, in proton-proton collision, a small production asymmetry  $A_p$  of B and  $\bar{B}$  mesons ( $\mathcal{O}(1\%)$ ) is expected.

#### 3.1 Lepton tagged sample

We have three lepton tagged signal samples: 1) muon tagged  $J/\psi K_S^0$ ,  $J/\psi \rightarrow \mu^+ \mu^-$ , 2) muon tagged  $J/\psi K_S^0$ ,  $J/\psi \rightarrow e^+ e^-$ , 3) electron tagged  $J/\psi K_S^0$ ,  $J/\psi \rightarrow \mu^+ \mu^-$ . The tag-electron was required to have  $p_T > 5 \text{ GeV}/c$ . One of the muons must satisfy the single muon trigger.

The analysis is the same as in [1]. The data samples were simulated with PYTHIA, using the old default parton distribution function EHLQ1. The  $K_S^0$  reconstruction efficiency has been studied in ATLAS using a full GEANT simulation [4]. The reconstruction efficiency was found to be 95% with a fake  $K_S^0$  rate of 6%. The  $J/\psi$  reconstruction has been documented in [1, 5]. In addition to  $p_T$  cuts and lepton identification, secondary vertex and mass cuts are used [1, 6]. The reconstructed B-lifetime is required to be greater than 0.5 ps and the  $p_T$  of the B greater than  $5 \text{ GeV}/c$ .

For the decay  $B \rightarrow J/\psi K_S^0 \rightarrow \mu^+ \mu^- K_S^0$ , the dominant background consists of a real  $J/\psi$  from a B decay, combined with a  $K_S^0$  from the fragmentation, assuming a hadron rejection factor of 50 in the muon spectrometer. For the decay  $B \rightarrow J/\psi K_S^0 \rightarrow e^+ e^- K_S^0$ , the dominant background comes from an (eh)-pair faking a  $J/\psi$ , combined with any  $K_S^0$ ,

assuming a hadron rejection factor of 30 in the TRT. The fake  $J/\psi$  background in the electron channel is due to the low  $p_T$  cut of 1  $\text{GeV}/c$  for electrons, and the large  $J/\psi$  mass window ( $600 \text{ MeV}/c^2$ ) due to bremsstrahlung. The fake  $J/\psi$  background from (eh)-pairs was not considered in [1]. The final results do not change significantly, however.

The final number of signal events is 21,120 for an integrated luminosity of  $10^4 \text{ pb}^{-1}$ . The breakdown of the signal and background events in the different event classes is given in Table 1. The result with the lepton tagged sample is  $\delta(\sin 2\beta)(\text{stat.}) = 0.021$  (time-int.).

Event class	$\mu$ -tags	e-tags
$N_S(J/\psi \rightarrow e^+e^- \oplus K_S^0)$	9,540	
$N_S(J/\psi \rightarrow \mu^+\mu^- \oplus K_S^0)$	6,220	5,360
$N_B(\text{real } J/\psi \rightarrow e^+e^- \oplus \pi^+\pi^-)$	1,170	
$N_B(\text{fake } e^+e^- \oplus \pi^+\pi^-)$	1,110	
$N_B(\text{fake eh} \oplus \pi^+\pi^-)$	1,550	
$N_B(\text{real } J/\psi \rightarrow \mu^+\mu^- \oplus \pi^+\pi^-)$	80	160
$N_B(\text{fake } \mu^+\mu^- \oplus \pi^+\pi^-)$	40	40
$N_B(\text{fake } \mu h \oplus \pi^+\pi^-)$	4	2

Table 1: Number of signal and background events in the lepton tagged  $B_d^0 \rightarrow J/\psi K_s^0$  samples.

Systematic uncertainties can be controlled using data from  $B^+ \rightarrow J/\psi K^+$  and  $B_d^0 \rightarrow J/\psi K^{0*}$  [7]: with an integrated luminosity of  $10^4 \text{ pb}^{-1}$ ,  $\delta D_{\text{tag}}/D_{\text{tag}} = 0.005$  (lepton tags),  $\delta A_p = 0.007$ . With decreased statistical errors in the control samples, these systematic uncertainties will decrease. For  $B_d^0 \rightarrow J/\psi K_S^0$ ,  $\delta D_{\text{back}}/D_{\text{back}} = 0.011$  (estimate). Combining these sources of systematic uncertainties, the following estimate is obtained:  $\delta(\sin 2\beta) (\text{syst.}) = \pm 0.012 \cdot \sin 2\beta \oplus 0.011$ .

### 3.2 $B^{**}$ and jet charge tagging

$B^{**}$  is a common label for orbitally excited  $L = 1$  state  $B$ 's. Theoretically, one expects a narrow and a wide doublet [8].  $B^{**}$  states have been observed at LEP [9]. The expected properties of charged  $B^{**}$  states are tabulated in Table 2.

Label	$j_q = L + S_q$	$J^P$	Mass [ $\text{GeV}/c^2$ ]	Width [ $\text{MeV}/c^2$ ]	Decays to
$B_1^+$	3/2	1 <sup>+</sup>	5.742	21	$B^{*0}\pi^+$
$B_2^{*+}$	3/2	2 <sup>+</sup>	5.754	25	$B^0\pi^+, B^{*0}\pi^+$
$B_0^{*+}$	1/2	0 <sup>+</sup>	5.630	100	$B^0\pi^+$
$B_1^{*+}$	1/2	1 <sup>+</sup>	5.642	100	$B^{*0}\pi^+$

Table 2: The charged  $B^{**}$  states. Masses and widths come from theoretical estimates and ALEPH data (unpublished).

The charge of the pion is a signature of the charge of the b quark:  $B^{**+} \rightarrow B^{0(*)}\pi^+$ ,

$B^{**-} \rightarrow \bar{B}^{0(*)}\pi^-$ , where  $B^{0(*)}$  denotes either a  $B^0$  or a  $B^{*0}$ . Even without a resonant structure, there is a correlation between the charge of pions nearby the  $B$  in phase space, and the flavour of the  $B$ . This correlation can be used to tag  $B$ 's on a statistical basis by using the jet charge as a tag. Jet charge techniques have been used successfully at LEP experiments for example for  $B$ -mixing measurements [10].

In ATLAS,  $B^{**}$  and jet charge tagging can be used to tag decays  $B_d^0 \rightarrow J/\psi X$ ,  $J/\psi \rightarrow \mu^+\mu^-$ , because the Level-1 trigger needs at least one muon passing the trigger requirements.  $B^{**}$  and jet charge tagging can thus be used in order to increase statistics for the  $\sin 2\beta$  measurement. In addition, systematic effects related to tagging can be checked by using the related decays  $B_d^0 \rightarrow J/\psi K^{*0}$  and  $B^+ \rightarrow J/\psi K^+$ .

Only jet charge tagging can be used for tagging decays of the type  $B_s^0 \rightarrow J/\psi X$ , since there is no phase space for the decay  $B_{u,d}^{**} \rightarrow B_s^0 K$ . Jet charge tagging can thus be used to increase statistics of  $\gamma$  measurement with  $B_s^0 \rightarrow J/\psi \phi$ , and possibly to increase statistics of  $x_s$  measurement with  $B_s^0 \rightarrow J/\psi K^{*0}$ , if reconstruction of this channel is otherwise feasible. There are expected to be heavier  $L = 2$  states, ' $B^{***} = B_3^*(6148) \rightarrow B_s K$ ,  $B_2(6148) \rightarrow B_s^* K$ ,  $B_s K^*$ ' [8]. These states have not been observed, but if these states were narrow and prominent, they could be useful for  $B_s^0$  tagging.

### 3.3 $B^{**}$ tagging of $\bar{B}_d^0 \rightarrow J/\psi X$ , $J/\psi \rightarrow \mu^+\mu^-$

$B^{**}$  decays were implemented in PYTHIA 5.7, using a tuning based on ALEPH data, with production probability  $P(b \rightarrow B_{u,d}^{**}/b \rightarrow B_{u,d}) = 0.3$ . The parton distribution function was the default one in PYTHIA 5.7, CTEQ2L. The simulation study was performed at particle level without resolution smearings [11]. The  $B\pi$  mass distribution of the simulated  $B^{**}$  sample is shown in Fig. 1.

The selection of the non-tagged  $\bar{B}_d^0 \rightarrow J/\psi K_S^0$  sample was the same as for lepton analysis, apart from the tag requirements. Normalizing to an integrated luminosity of  $10^4 \text{ pb}^{-1}$ , a sample of 59,000 reconstructed, untagged  $\bar{B}_d^0 \rightarrow J/\psi K_S^0$  events was obtained after the selection cuts.

The tag-pion was first required to be consistent with coming from the primary vertex by requiring that the impact parameter was smaller than  $250 \mu\text{m}$ . The tagging quality factor can be defined as  $Q_{\text{tag}} = \varepsilon_{\text{tag}} D_{\text{tag}}^2$ , where  $\varepsilon_{\text{tag}}$  is the tagging efficiency.  $Q_{\text{tag}}$  was maximized by optimizing the minimum  $p_T$  of the pion, maximum  $B\pi$  invariant mass, maximum distance of the pion from the  $B$ ,  $\Delta r = \sqrt{\Delta\eta^2 + \Delta\phi^2}$ , and the maximum number of allowed pion candidates,  $n_{\text{cand}}$ . To select the tag pion in case of multiple candidates passing the cuts, a few selection algorithms were tried: selection based on 1) maximum  $p_L$  with respect to the  $B$ , 2) maximum  $\cos\theta^*$ , where  $\theta^*$  is the angle between the pion and the  $B^{**}$  boost direction, after a boost to  $B\pi$  rest frame, and 3)  $M(B\pi)$  closest to  $M(B^{**})$ .

Optimal cuts for the tag pion were found to be:  $p_T > 1 \text{ GeV}/c$ ,  $\Delta r < 0.5$ ,  $M(B\pi) < 6.0 \text{ GeV}/c^2$ ,  $n_{\text{cand}} = 1$ . Since events with only one tag-pion candidate were accepted, there was no need for additional selection criteria. The  $B\pi$  mass distribution of the tagged events, using the optimized cuts, is shown in Fig. 2. Results with optimal cuts were:

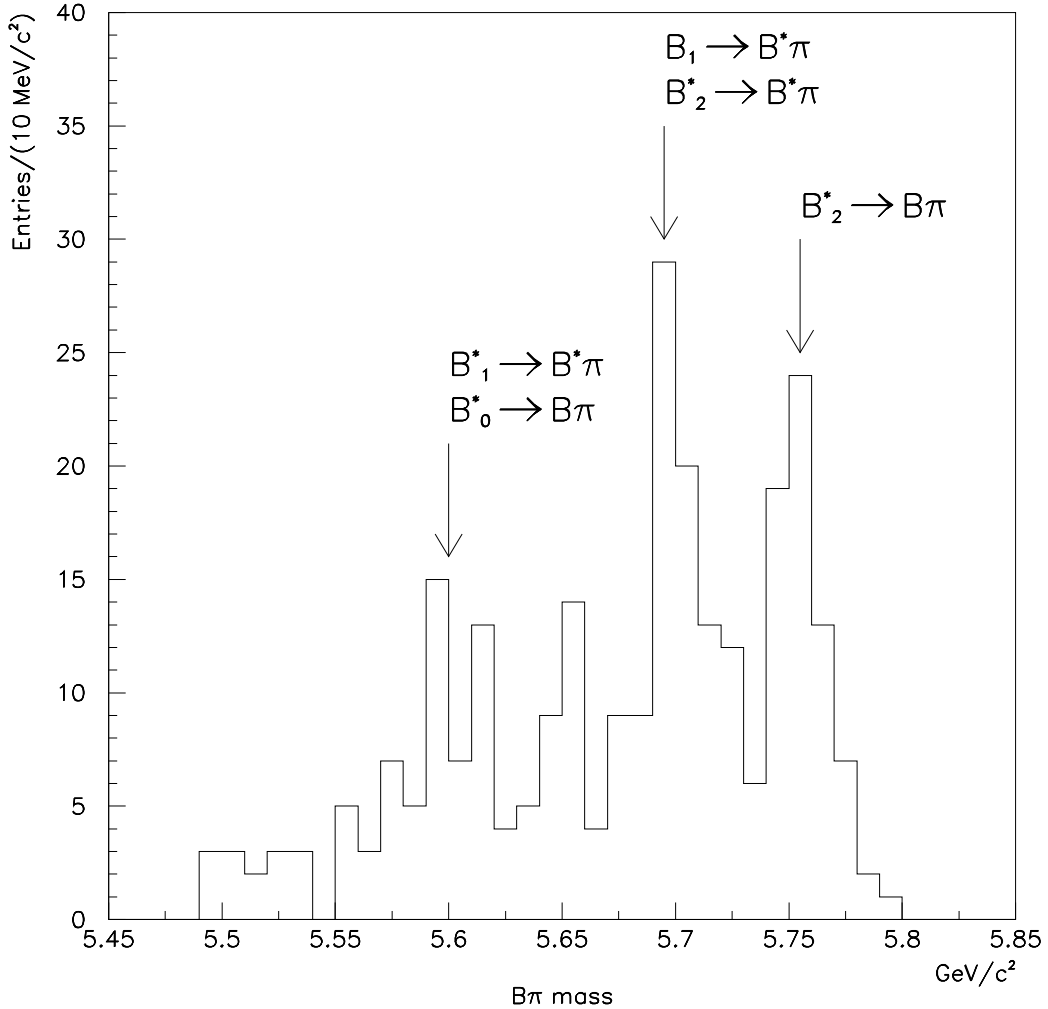


Figure 1: The  $B\pi$  mass spectrum of the simulated  $B^{**}$  sample. In  $B^*$  final states, the unreconstructed photon produces a mass shift of about  $46 \text{ MeV}/c^2$ .

$$W_{\text{tag}} = 0.28 \pm 0.02 \rightarrow D_{\text{tag}} = 0.44$$

$$\varepsilon_{\text{tag}} = 0.26 \pm 0.01$$

$$Q_{\text{tag}} = 0.052 \pm 0.010$$

Assuming the same S/B as for the lepton-tagged sample,  $\delta(\sin 2\beta)(\text{stat.}) = 0.032 \pm 0.003$ . When considering the channel  $J/\psi \rightarrow \mu^+\mu^-$ , the lepton-tag analysis showed that

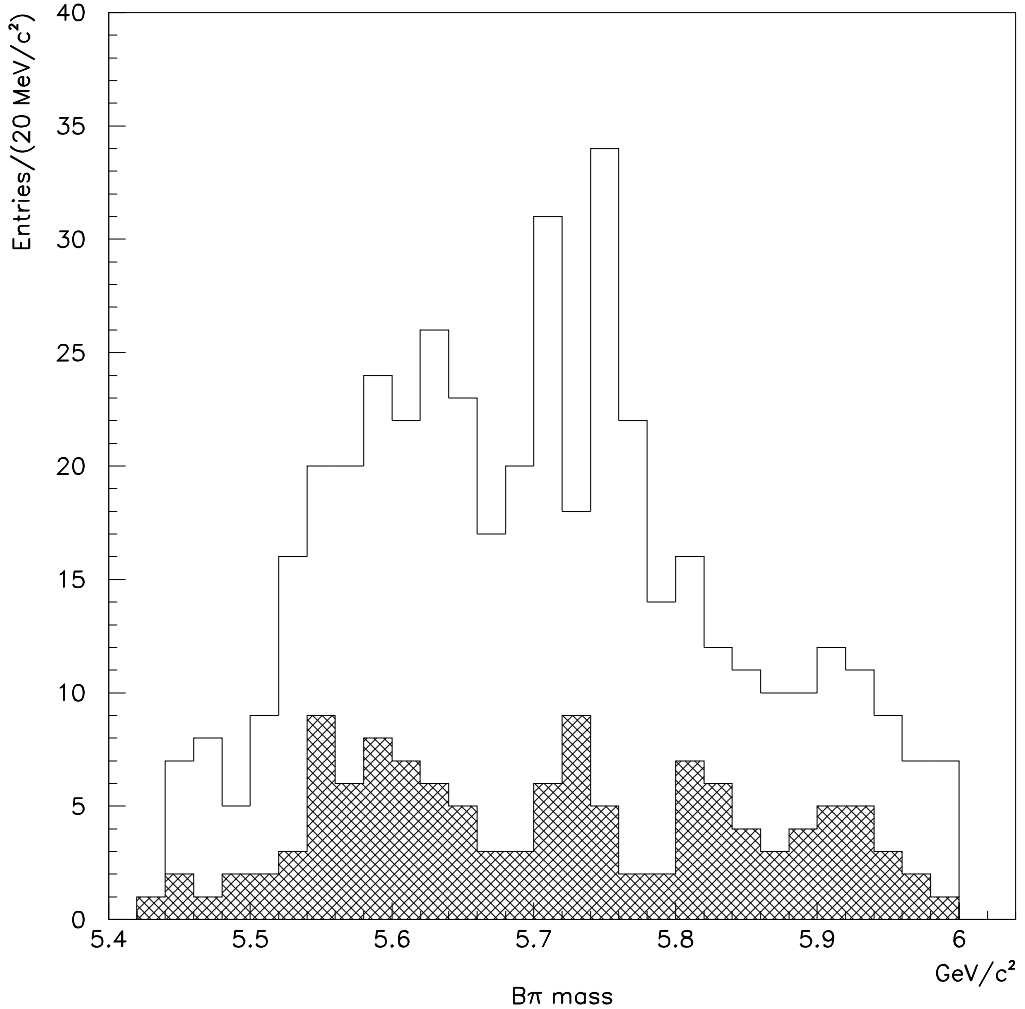


Figure 2: The  $B\pi$  mass distribution of the tagged events. The hatched histogram shows the wrong-sign combinations and the white histogram shows the right-sign combinations. Of the 1688 events passing the reconstruction cuts, 320 were tagged right and 122 wrong.

the dominant background originates from real  $J/\psi$ 's, since fake background is reduced by the high  $p_T$  cuts of the muons, and the good mass resolution. The lifetime cut of the  $B$  should suppress background from prompt  $J/\psi$ 's, and work is in progress to verify this.

For comparison, the wrong-tag rate with lepton tags is  $W_{\text{tag}} = 0.22$ , giving  $D_{\text{tag}} = 0.56$ . The lepton tagging efficiency includes trigger efficiencies, since the tag lepton is part of the trigger. The theoretical maximum for the tagging efficiency would be about 0.20 (from semileptonic branching ratios).

### 3.4 Jet charge tagging of $\bar{B}_d^0 \rightarrow J/\psi K_S^0, J/\psi \rightarrow \mu^+ \mu^-$

The simulation sample for the study of jet charge tagging was the same as for the  $B^{**}$  analysis, and the same selection cuts were used [12]. Two different tagging methods were tried. In same-side jet tagging, the tag was defined as the jet around the  $J/\psi K_S^0$ . The tagging variable was the jet charge  $Q_s$ . A jet with  $Q_s < -c$  was defined as originating from a  $\bar{B}_d^0$ , and if  $Q_s > c$ , the jet was defined to originate from a  $B_d^0$ . In the same-side jet analysis, the jet cone size  $\Delta r$ , the  $p_T$  cut for the particles in the cone, and the charge cut-value  $c$  defining the flavour of the  $B$  were optimized to maximize the  $Q_{\text{tag}}$ .

The other method studied was two-jet tagging, in which both the same side jet and the ‘other b-jet’ were used for tagging. The tagging variable was defined as the charge difference of the two jets,  $dQ = \langle Q_s - Q_o \rangle$ . Contrary to LEP, at LHC it is not obvious which is the other b-jet. Here, the highest- $E_T$  jet (excluding the same side jet) was taken as the other b-jet but the identification was correct only in 25% of the cases. We can, however, expect to improve this by optimizing the jet reconstruction algorithm and including b-tagging for the other jet. For comparison, the other b-jet was also identified using the Monte Carlo simulation history in order to have an idea of the optimal performance.

The jet charge was calculated as:

$$Q_{\text{jet}} = \frac{\sum_{i=1}^n q_i (p_i)_T^a}{\sum_{i=1}^n (p_i)_T^a} \quad (1)$$

where  $(p_i)_T$  is the transverse momentum of particle  $i$  vs. beam direction. Exponent  $a$  was optimized along other parameters. Algorithms based on longitudinal momentum  $p_L$  and rapidity  $y$  along the jet axis were tried as well, with similar results.

Best results were obtained with two-jet tagging using the  $p_T$ -based algorithm for calculating the jet charges. The distribution of the tagging variable  $dQ$  is shown in Fig. 3. The  $Q_{\text{tag}}$  was maximal with the following parameters:  $\Delta r=0.7$ ,  $p_T > 0.5 \text{ GeV}/c$ , charge cut value  $c=0.4$ , exponent  $a=1.25$ .

The results were:

$$W_{\text{tag}} = 0.34 \rightarrow D_{\text{tag}} = 0.32$$

$$\varepsilon_{\text{tag}} = 0.32$$

$$Q_{\text{tag}} = 0.033 \pm 0.009$$

Assuming the same S/B as for the lepton-tagged sample,  $\delta(\sin 2\beta)(\text{stat.}) = 0.040 \pm 0.003$ .

Similar results were obtained with same-side jet tagging, using the rapidity-based algorithm for the jet-charge calculation. With optimal parameters  $\Delta r=0.7$ ,  $p_T > 0.5 \text{ GeV}/c$ ,  $c=0.2$ , the tagging quality factor  $Q_{\text{tag}}$  was 0.031.

For comparison, the result with ideal two-jet tagging (the other b-jet always found correctly) was:  $Q_{\text{tag}} = 0.042 \pm 0.009$ .

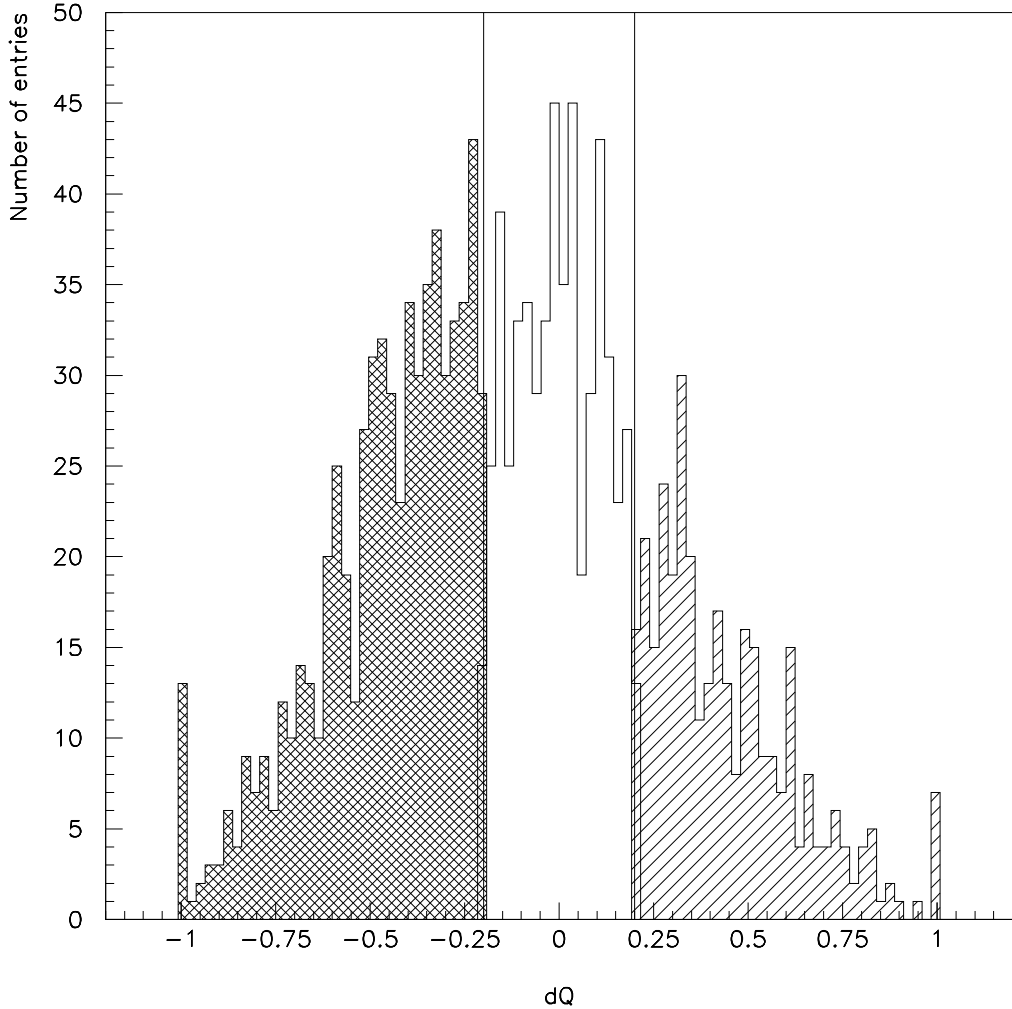


Figure 3: Distribution of the charge difference between the two jets,  $dQ$ . Here, events with  $dQ < -0.2$  are defined as tagged right (cross-hatched region) and jets with  $dQ > 0.2$  are tagged wrong (hatched region), resulting in a wrong tag fraction of about 34%.

### 3.5 Combined results

Estimates of the ATLAS measurement accuracy of  $\sin 2\beta$  are summarized in Tables 3 and 4. With the  $B^{**}$ -tagged sample, a statistical precision of  $\pm 0.032$  is obtained, which is comparable to the precision obtained with the muon-tagged sample with  $J/\psi \rightarrow \mu^+\mu^-$  in the final state ( $\pm 0.036$ ). There is a large overlap between the event samples selected by the  $B^{**}$  and jet charge tags, while the overlap with the lepton-tagged sample and the

other samples should be small. Work is in progress to combine the different samples in an optimal way.

Parameter	$\mu$ -tags	e-tags
$N_S(e^+e^-K_S^0)$ rec.	9,540	
$N_S(\mu^+\mu^-K_S^0)$ rec.	6,220	5,360
$N_S$		21,120
$N_B(e^+e^- \oplus \pi^+\pi^-)$	3,820	
$N_B(\mu^+\mu^- \oplus \pi^+\pi^-)$	120	200
$\sqrt{D}_{\text{back}}$		0.91
$D_{\text{tag}}$		0.56
$D_{\text{int}}$		0.63
$\delta(\sin 2\beta)$ (stat.)		0.018 (time-dep.)
$\delta(\sin 2\beta)$ (stat.)		0.021 (time-int.)
$\delta(\sin 2\beta)$ (syst.)		$0.012 \cdot \sin 2\beta \oplus 0.011$ (time-int.)

Table 3: Summary on  $\sin 2\beta$  with  $10^4 \text{ pb}^{-1}$ : lepton tags.

Parameter	B <sup>**</sup> -tags	Jet charge tags
$N_S(\mu^+\mu^-K_S^0)$ rec., untagged		59,000
$N_S(\mu^+\mu^-K_S^0)$ rec., tagged	15,340	18,760
$\sqrt{D}_{\text{back}}$ (assumed)		0.91
$D_{\text{tag}}$	0.44	0.32
$D_{\text{int}}$		0.63
$\delta(\sin 2\beta)$ (stat.)	0.032 (time-int.)	0.040 (time-int.)

Table 4: Summary on  $\sin 2\beta$  with  $10^4 \text{ pb}^{-1}$ : B<sup>\*\*</sup> and jet charge tags.

## 4 Other CP-violation measurements

ATLAS capabilities of measuring  $\sin 2\alpha$  have been investigated in [1, 13]. With an integrated luminosity of  $10^4 \text{ pb}^{-1}$ , 7,120 signal events are expected, with a background of 6,475 events from other exclusive two- or three-body B-decays, and 565 events from combinatorial background. Neglecting the penguin contributions to the decay, the statistical error on  $\sin 2\alpha$  has been estimated to be  $\pm 0.043$ . The experimental systematic uncertainty is dominated by the large background, since ATLAS does not have charged hadron identification. Assuming a 20% systematic uncertainty for the level of background, the systematic uncertainty of  $\sin 2\alpha$  is  $\pm 0.10 \cdot \sin 2\alpha \oplus 0.011$ .

Since ATLAS is not expected to be able to reconstruct decays  $B_d^0 \rightarrow \pi^0\pi^0$  and  $B^\pm \rightarrow \pi^\pm\pi^0$ , ATLAS cannot measure the parameter  $\rho = A_P/A_T$ , which is the ratio of penguin to tree amplitudes. If  $\rho$  is measured elsewhere, or calculated reliably, ATLAS should

be able to measure  $\sin 2\alpha$  despite of the penguin effects. If one pessimistically assumes  $\rho = 0.2 \pm 0.2$ , the theoretical systematic uncertainty can be very large,  $\delta \sin 2\alpha \simeq 0.1\text{-}0.3$ .

In the decay channel  $B_s^0 \rightarrow J/\psi\phi$ , a small asymmetry is expected in the Standard Model,

$$A(t) \propto D \cdot 2|V_{cd}||V_{ub}/V_{cb}| \cdot \sin \gamma \sin \Delta m_s t \simeq 0.03 \cdot D \cdot \sin \gamma \sin \Delta m_s t. \quad (2)$$

New physics phenomena, contributing to B-mixing, could enhance the asymmetry substantially.

A study of this decay channel was documented in [1, 14]. With an integrated luminosity of  $10^4 \text{ pb}^{-1}$ , a signal of 15,000 lepton-tagged events is expected, with a background of 3,000 events. The precision with which the asymmetry can be measured depends on the value of  $x_s$ , because a time-dependent measurement of the asymmetry is mandatory due to the expected large value of  $x_s$ . Assuming  $x_s = 10$ ,  $\delta(A_{\text{obs}}) = 0.025$ , and with  $x_s = 25$ ,  $\delta(A_{\text{obs}}) = 0.06$ . The signal statistics could be increased with jet charge tagging.

## 5 Measurement of $x_s$

In addition to the angles of the unitarity triangle, measurements of the lengths of the sides provide us with complementary information about the triangle. The length of the side  $|V_{td}|$  is least well-known of the sides. The mixing parameter  $x_d$  is proportional to  $|V_{td}|^2$ , but inferring the value of  $|V_{td}|^2$  from  $x_d$  is hampered by hadronic uncertainties. To large extent, these uncertainties cancel, when considering the ratio of the mixing parameters,  $x_s/x_d \propto |V_{ts}/V_{td}|^2$ .

The mixing parameter  $x_s$  has not been measured yet. The Standard Model predicts it to be in the range 10-30, and the present lower limit from LEP is  $x_s > 11.1$  [15].

The following decay channels were studied for  $x_s$  measurement in ATLAS:  $B_s^0 \rightarrow D_s^- \pi^+$ ,  $D_s^- \rightarrow \phi^0 \pi^-$ ,  $\phi^0 \rightarrow K^+ K^-$  and  $B_s^0 \rightarrow D_s^- a_1^+$ ,  $D_s^- \rightarrow \phi^0 \pi^-$ ,  $\phi^0 \rightarrow K^+ K^-$ ,  $a_1^+ \rightarrow \rho^0 \pi^+$ ,  $\rho^0 \rightarrow \pi^+ \pi^-$ .

### 5.1 $B_s^0 \rightarrow D_s^- \pi^+$

The first level trigger for this decay channel is a single muon coming from the semileptonic decay of the accompanying b. The trigger muon also serves as a tag defining the flavour of the  $B_s^0$  at production. The second level trigger is a  $D_s$  mass trigger.

Three-dimensional vertex fits of  $D_s^-$  and  $B_s^0$  were performed [16]. From full simulation, the decay time resolution of the B was found to be  $\sigma_t(B) = 0.069 \pm 0.008 \text{ ps}$ . The  $B_s^0$  mass resolution was  $33 \text{ MeV}/c^2$ , and the  $D_s^-$  mass resolution  $10 \text{ MeV}/c^2$ .

After the reconstruction cuts, and including trigger and reconstruction efficiencies, 3,640 reconstructed events were obtained, assuming an integrated luminosity of  $10^4 \text{ pb}^{-1}$ .

Backgrounds studied were: related B decays  $B_d^0 \rightarrow D_s^- \pi^+$ ,  $B_d^0 \rightarrow D^- \pi^+$ , and  $\Lambda_b \rightarrow \Lambda_c^+ \pi^-$ ,  $\Lambda_c^+ \rightarrow p K^- \pi^+$ . Combinatorial background was checked as well. No significant background from these sources was found, and in the consequent analysis, the signal-to-background ratio was assumed to be 1.6, which should be an upper limit for the background.

## 5.2 $B_s^0 \rightarrow D_s^- a_1^+(1260)$

The trigger for this channel is as for the decay  $B_s^0 \rightarrow D_s^- \pi^+$ . Three-dimensional vertex fits were performed to reconstruct  $D_s^-$ ,  $a_1^+$  and  $B_s^0$  [17]. To find  $a_1^+$ , further cuts were applied on  $\Delta\phi_{\pi\pi}$ ,  $\Delta\Theta_{\pi\pi}$ ,  $|M_{\pi\pi} - M_\rho|$  and  $|M_{\pi\pi\pi} - M_{a_1}|$ . The decay time resolution was found to be 0.064 ps.

No significant background was found from:  $B_d^0 \rightarrow D_s^- a_1^+$ ,  $B_d^0 \rightarrow D^- a_1^+$ ,  $\Lambda_b \rightarrow \Lambda_c^+ \pi^-$ ,  $\Lambda_c^+ \rightarrow p K^- \pi^+ \pi^- \pi^+$ , and combinatorial background.

After the reconstruction cuts, and including trigger and reconstruction efficiencies, 1,230 reconstructed events were obtained.

## 5.3 The $x_s$ reach

The asymmetry between the decay time distributions of unmixed (++) and mixed B's (+-) is:

$$A(\tau) = \frac{dn(++)/d\tau - dn(+-)/d\tau}{dn(++)/d\tau + dn(+-)/d\tau} = D \cos(x_s \tau / \tau_{Bs}), \quad (3)$$

where  $D$  is the product of all dilution factors,  $D_{\text{tag}} = 0.56$ ,  $D_{\text{back}} = 0.61$  (S/B=1.6),  $D_{\text{time}}$  (dependent on  $x_s$ ).

In [1], we used the power spectrum of Fourier transform to obtain the value of  $x_s$  from the asymmetry. This kind of transformation can be applied to any type of asymmetry function.

A refined fitting method, an amplitude fit, has been proposed in [18]. The amplitude fit is equivalent to using a Fourier cosine transform. In this method, a cosine-function, or an even function in more general case, is explicitly required.

The amplitude fit is performed in the following way:  $x_s$  values are scanned, and for every fixed  $x_s$ , the amplitude  $D$  in the expression  $D \cos(x_s \tau / \tau_{Bs})$  is fitted. The  $B_s^0$  lifetime is fixed to its measured value. The  $x_s$  value which gives the maximum fitted amplitude  $D$ , is then the measured value.

The reachable  $x_s$  range was defined by repeating the ‘experiment’ 1,000 times, and in 95% of the cases, a correct answer was required from the amplitude fit. Combining the two decay modes, it was found that ATLAS can measure  $x_s$  values up to 37 with one year’s statistics ( $10^4 \text{ pb}^{-1}$ ). The results are shown in Fig. 4 for samples generated with  $x_s = 37$ .

Finally, ATLAS will also be able to measure  $x_d$  with a good precision, and thus we can measure independently the ratio  $x_s/x_d$ .

## 6 Rare decays $B \rightarrow \mu^+ \mu^- (X)$

LHC provides a sufficient  $b\bar{b}$  production rate to study rare decays  $B \rightarrow \mu^+ \mu^- (X)$ . The decays are easily triggered with a low-rate di-muon trigger. The analysis cuts are based on secondary vertex requirements and B decay kinematics [19, 20].

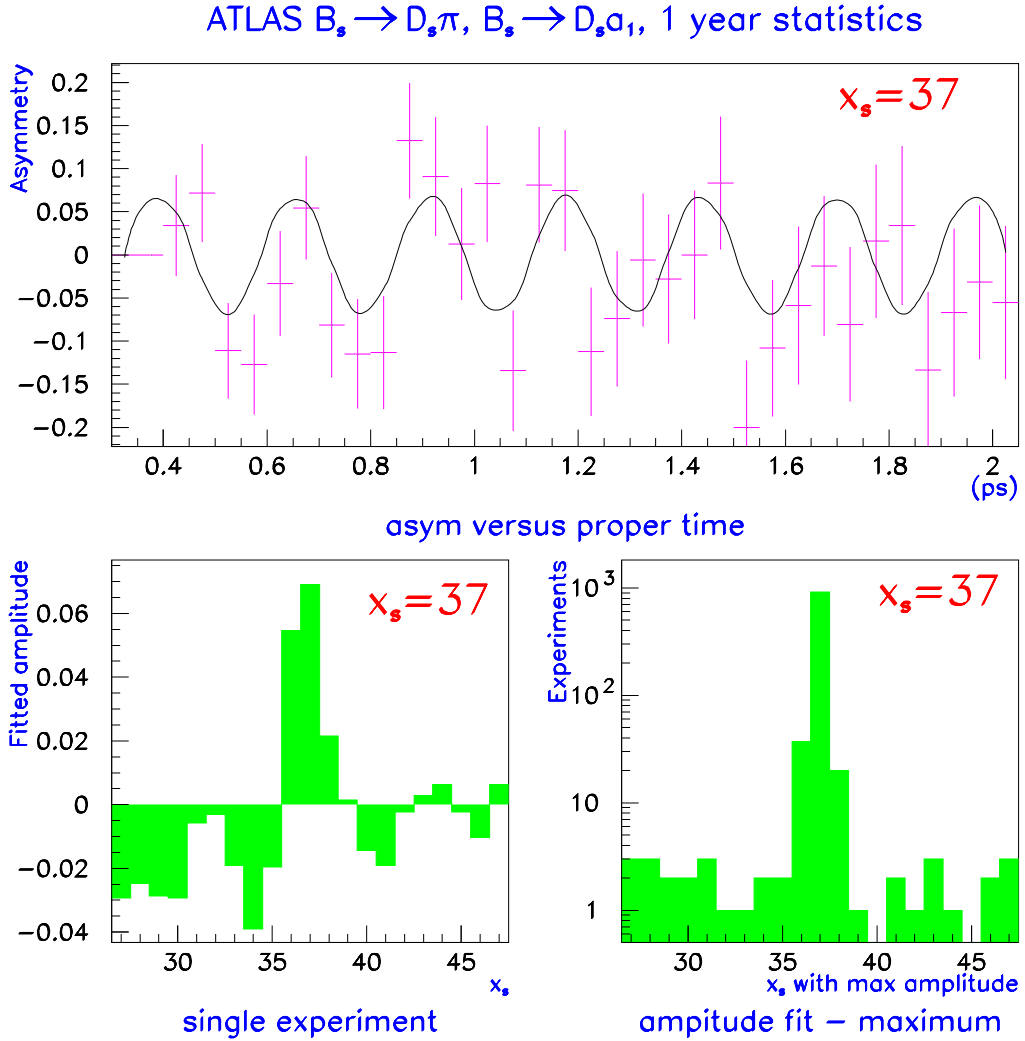


Figure 4: a) Asymmetry versus proper time for  $x_s=37$ . b) Result of the amplitude fit with  $x_s$  scan. c) Distribution of the  $x_s$  corresponding to the maximum amplitude, when the experiment was repeated 1,000 times.

With an integrated luminosity of  $10^4 \text{ pb}^{-1}$ , the upper limit to the branching ratio of the decay  $B_s^0 \rightarrow \mu^+ \mu^-$  can be established to be  $\text{BR}(B_s^0 \rightarrow \mu^+ \mu^-) = 2.5 \times 10^{-9}$  at 95% C.L.. The Standard Model predicts a branching ratio  $\mathcal{O}(10^{-9})$ . After two low-luminosity LHC-years, a two-standard-deviation signal can be seen.

For the decay  $B_d^0 \rightarrow \mu^+ \mu^-$ , the Standard Model prediction for the branching ratio is  $\mathcal{O}(10^{-10})$ . An upper limit of  $\text{BR}(B_d^0 \rightarrow \mu^+ \mu^-) = 6.6 \times 10^{-10}$  can be established at 95% C.L..

The ratio of the branching ratios of the decays  $B_d^0 \rightarrow \rho^0 \mu^+ \mu^-$  and  $B_d^0 \rightarrow K^{*0} \mu^+ \mu^-$  provides us with an independent measurement of the CKM matrix elements:

$$\frac{\text{Br}(B_d^0 \rightarrow \rho^0 \mu^+ \mu^-)}{\text{Br}(B_d^0 \rightarrow K^{*0} \mu^+ \mu^-)} = k_d \frac{|V_{td}|^2}{|V_{ts}|^2}, \quad (4)$$

where  $k_d = (F^{B_d^0 \rightarrow \rho^0}/F^{B_d^0 \rightarrow K^{*0}})^2$  is the ratio of form factors squared. Ratio of the form factors is calculable with an error of 5 - 10%.

In the decay channel  $B_d^0 \rightarrow K^{*0} \mu^+ \mu^-$ , a signal of 2,450 events is expected assuming the Standard Model branching ratio, over a combinatorial background of 420 events. In the decay channel  $B_d^0 \rightarrow \rho^0 \mu^+ \mu^-$ , 330 signal events (produced according to the branching ratio predicted by the Standard Model) are expected to be observed over a background of 860 events, consisting of both combinatorial background and reflection from  $B_d^0 \rightarrow K^{*0} \mu^+ \mu^-$ .

## 7 Other B-physics topics with ATLAS

Among other B-physics topics, B-baryons and  $B_c$  mesons have been studied in ATLAS. The polarization of  $\Lambda_b$  is expected to be measured with a statistical accuracy of 0.008, using the decay mode  $J/\psi \Lambda$  [21]. The  $\Xi_b$  polarization will be measured with a statistical accuracy of 0.14, using the same decay mode. In decay mode  $B_c \rightarrow J/\psi \pi$ , a signal of about 4,000 events with a 14-standard-deviation significance can be established with  $10^4 \text{ pb}^{-1}$  of data [22].

## 8 Conclusions

ATLAS will be very competitive in the measurement of  $\sin 2\beta$ , due to the possibility to use low- $p_T$  electrons, good vertex resolution, and versatile tagging methods. In addition, ATLAS will contribute to the measurements of other angles of the unitarity triangle: angles  $\alpha$  and  $\gamma$ .

ATLAS will be able to measure a side of the triangle independently. In addition to the measurement of  $x_d$ , the measurement of  $x_s$  will be possible by utilizing the dedicated vertex layer close to the beam pipe.

ATLAS will have access to rare decays  $B \rightarrow \mu^+ \mu^- (X)$ , due to the efficient muon trigger and identification, and vertexing. These decays provide us with a Standard Model (in)consistency test. ATLAS will also have access to rare B-hadrons such as  $B_c$  and baryons with more than one heavy quark, which will test heavy quark models.

## 9 Acknowledgement

Special thanks to CERN 1995 summer students Patrik Johnsson and Lena Leinonen for their contributions to the results presented in this paper.

## References

- [1] ATLAS Technical Proposal, CERN/LHCC/94-43, LHCC/P2 (15 December 1994).
- [2] P. Eerola, Nucl. Instr. and Methods A 333 (1993) 73;  
P. Eerola et al., Nucl. Instr. and Methods A 351 (1994) 84;  
A. Nisati, Nucl. Instr. and Methods A 368 (1995) 109.
- [3] F. Gianotti, ‘Tagging of low- $p_T$  electrons from b decays with the ATLAS electromagnetic calorimeter’, ATLAS Internal Note PHYS-NO-049 (1995).
- [4] ATLAS Collaboration, CERN/LHCC/93-51 (1993).
- [5] I. Gavrilenko, ‘Reconstruction of  $J/\psi$  to electron decay’, ATLAS Internal Note PHYS-NO-055 (1994).
- [6] P. Eerola et al., ‘An evaluation of the statistical error on  $\sin 2\beta$  using the ATLAS detector’, ATLAS Internal Note PHYS-NO-047 (1994).
- [7] P. Eerola et al., ‘Asymmetries in B decays and their experimental control’, ATLAS Internal Note PHYS-NO-054 (1994).
- [8] E.J. Eichten, C.T. Hill and C. Quigg, ‘Orbitally Excited Heavy-Light Mesons Revisited’, FERMILAB-CONF-94/118-T (1994).
- [9] R. Akers et al., OPAL Collaboration, Zeit. Phys. C66 (1995) 19;  
P. Abreu et al., DELPHI Collaboration, Phys. Lett. B345 (1995) 598;  
D. Buskulic et al., ALEPH Collaboration, Zeit. Phys. C69 (1996) 393.
- [10] R. Akers et al., OPAL Collaboration, Phys. Lett. B327 (1994) 411;  
D. Buskulic et al., ALEPH Collaboration, Phys. Lett. B356 (1995) 409;  
P. Abreu et al., DELPHI Collaboration, ‘Measurement of the  $B_d^0$  oscillation frequency using kaons, leptons and jet charge’, CERN-PPE/96-06 (1996), subm. to Zeit. Phys. C.
- [11] P. Johnsson, ‘A study of the use of the decay  $B^{**+} \rightarrow B^0(*)\pi^+$  for  $B^0 - \bar{B}^0$  tagging in ATLAS’, ATLAS Internal Note PHYS-NO-073 (1995).
- [12] L. Leinonen, ‘A study of B-tagging in ATLAS using jet charge techniques’, ATLAS Internal Note PHYS-NO-082 (1996).
- [13] P. Camarri et al., ‘A study of the decay  $B_d^0 \rightarrow \pi^+\pi^-$ ’, ATLAS Internal Note PHYS-NO-056 (1994).
- [14] M.C. Cousinou and L. Pouit, ‘ATLAS sensitivity to CP violation in the channels  $B_s^0 \rightarrow J/\psi\phi$  and  $B_s^0 \rightarrow D_s^\pm K^\mp$ ’, ATLAS Internal Note PHYS-NO-046 (1994).
- [15] C. Zeitnitz, these proceedings.

- [16] P. Eerola, S. Gadomski and B. Murray, ‘ $B_s^0$  mixing measurement in ATLAS’, ATLAS Internal Note PHYS-NO-039 (1994).
- [17] A.V. Bannikov, G.A. Chelkov and Z.K. Silagadze, ‘ $B_s^0 \rightarrow D_s^- a_1^+$  decay channel in the  $B_s^0$ -mixing studies’, ATLAS Internal Note PHYS-NO-072 (1995).
- [18] H.-G. Moser and A. Roussarie, ‘Mathematical Methods for  $B^0 - \bar{B}^0$  Oscillation Analyses’, Aleph Technical Note PUB 96-005, submitted to Nucl. Instr. and Methods.
- [19] D. Melikhov et al., ‘Purely muonic decays of B-mesons’, ATLAS Internal Note PHYS-NO-045 (1994).
- [20] D. Melikhov, F. Rizatdinova and L. Smirnova, ‘Investigation of rare semimuonic B-decays’, ATLAS Internal Note PHYS-NO-083 (1995).
- [21] J. Hrivnac, R. Lednický and M. Smizanska, J. Phys. G 21 (1995) 629.
- [22] F. Albiol et al., ‘Searching for  $B_c$  mesons in ATLAS’, ATLAS Internal Note PHYS-NO-058 (1994);  
results updated in R. Perez-Ochoa, ‘Status of  $B_c$  analysis’, ATLAS Internal Presentation B-PHY-TR-49 (1996).